Improving the sensitivity and bandwidth of time-of-flight scanning LIDAR using few-mode preamplified receivers

Rachel Sampson,* Huiyuan Liu, and Guifang Li
University of Central Florida, The College of Optics and Photonics,
Optical Fiber Communications Group, CREOL, Orlando, Florida, United States

Abstract. Within telecommunications, it is well established that optical preamplified receivers offer better sensitivity than linear-mode (LM) avalanche photodiodes (APDs) for direct-detection measurements. Long-range light detection and ranging (LiDAR), however, has predominantly made use of LM APDs for detection. This discrepancy arose due to the high coupling loss between the multimode return signals in LiDAR and single-mode optical preamplifiers. Recently, few-mode (FM) optical preamplifiers have been experimentally demonstrated, which solve this modal mismatch. We evaluate the applicability of FM preamplified receivers to long-range pulsed LiDAR in comparison with currently deployed LM APDs by considering the two receivers' noise, gain, and bandwidth characteristics. We show that FM preamplified receivers can offer an improvement in both receiver signal-to-noise ratio and bandwidth. © *2022 Society of Photo-Optical Instrumentation Engineers (SPIE)* [DOI: 10.1117/1.OE.61.12.123106]

Keywords: light detection and ranging; optical amplifiers; fiber amplifiers; erbium; laser radar; fiber applications.

Paper 20220972G received Aug. 30, 2022; accepted for publication Dec. 7, 2022; published online Dec. 31, 2022.

1 Introduction

Light detection and ranging (LiDAR) has seen an influx of interest in recent years, with applications in autonomous vehicles, industrial manufacturing, and topographic mapping.[1–4] In LiDAR, light is emitted, collected after partial reflection off an object, and characterized to determine how far the light travelled and thereby the distance to the reflecting object. One of the simplest and most popular implementations is time-of-flight (ToF) LiDAR.[2] In ToF LiDAR, light's travel time to and from a target (t) is measured, and the speed of light (c) is used in conjunction with $2L = ct$ to calculate the distance to the target. A schematic of LiDAR is shown in Fig. 1.

For long-range (150+ m) LiDAR, linear-mode (LM) avalanche photodiodes (APDs) are the preferred detector type.[5–7] LM APDs offer improved sensitivity compared with PIN photodiodes.[7] They also offer greater tolerance to background noise and shorter dead times than single-photon detectors.[7] However, the measurement speed of high-gain LM APDs is restricted due to their fixed gain-bandwidth product.[8] Optical preamplified receivers, using erbium-doped fiber amplifiers (EDFAs) and PIN photodiodes, offer higher bandwidth and superior sensitivity compared with LM APDs.[9,10] However, until recently, optical amplifiers were largely single mode (SM), which led to high coupling loss for return speckle patterns and made them unsuitable for LiDAR.[3]

Speckle is unavoidable in LiDAR systems even when SM sources are used at the transmitter to provide diffraction-limited illumination.[11,12] Speckle patterns arise when coherent light reflects off a rough surface, manifesting as a collection of bright and dark regions, as shown in Fig. 1. Each speckle pattern is the result of a superposition of spatial modes, among which only the fundamental mode can be efficiently coupled into SM fibers. Variations in intensity over the beam profile produce fluctuations in the received power for SM receivers, leading to

*Address all correspondence to Rachel Sampson, rachel.sampson@knights.ucf.edu

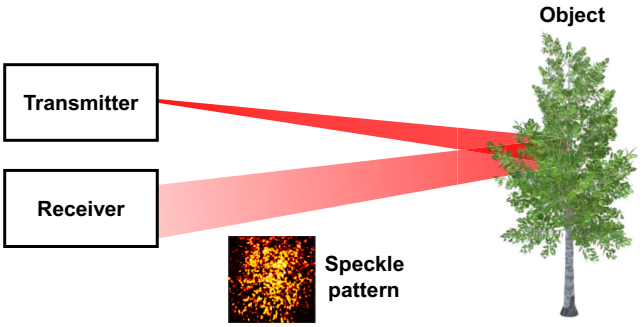

Fig. 1 Schematic of LiDAR where reflection off a rough surface produces a speckle pattern at the receiver.

degraded and nonuniform system performance.[11] However, since speckle intensity is an uncorrelated random variable, power variations can be mitigated by averaging over multiple speckles.[11,13,14] This averaging can occur in time for low sampling rate applications or space for high sampling rate applications.[11,13,14] Recent advances in space-division multiplexing have led to the demonstration of few-mode (FM) EDFAs, which collect multiple spatial modes contained within speckle patterns, thereby reducing the coupling loss of optical amplifiers and making them well-suited for LiDAR.[15–17]

In this paper, we propose and evaluate FM optical preamplified receivers as a new receiver architecture for long-range LiDAR. We focus our comparison on pulsed scanning LiDAR systems operating at 1550 nm due to their simplicity and high power budget.[7,15,18] Previous experimental demonstrations showed an order of magnitude improvement in signal-to-noise ratio (SNR) performance between a FM optical preamplified receiver and an LM APD.[15] This paper builds off the preliminary investigation presented in Ref. 15 and provides the framework to evaluate the performance of FM optical preamplified receivers as detectors for long-range pulsed LiDAR. We found that FM optical preamplified receivers can offer improved SNRs compared with the currently dominant LM APDs. Furthermore, we show that the high bandwidth required for long-range, high-resolution scanning LiDAR systems can be satisfied by the proposed FM optical preamplified receivers but not by LM APDs.

2 Receiver SNR Calculations

Both LM APDs and optical preamplified receivers use signal amplification to achieve superior sensitivity to PIN photodiodes. In the absence of gain, both receivers are thermal-noise limited. However, through amplification, the signal is increased without increasing the thermal noise. In LM APDs, received photons excite primary carriers that then cause an avalanche of secondary carrier generation. While in optical amplifiers, the optical signal is directly enhanced via stimulated emission and then the amplified signal participates in electron generation. The gain provided through amplification can improve the receiver SNR that is defined as

$$\mathrm{SNR} = I^2/\sigma_n^2, \tag{1}$$

where I is the received signal current and σ_n^2 is the total noise variance.[9,10] However, the amplification process is not noiseless, shot noise is increased in LM APDs, and amplified spontaneous emission (ASE) is produced in preamplified receivers. The following discussions focus on the contribution of the receiver to the SNR.

2.1 *Avalanche Photodiodes*

For the rest of the paper, LM APDs will be referred to as APDs for simplicity. The performance statistics of APDs are well-established and are summarized in this section. [9,10] In APDs, the received signal current is

$$I = R\langle M\rangle P_{\text{rec}}, \tag{2}$$

where R is the photodiode responsivity, $\langle M\rangle$ is the average APD gain, and P_{rec} is the received optical power.[9,10] At low light levels, there are two dominant noise sources in APDs, such as shot and thermal noises. To obtain the total noise variance, the two noise variances are added.

The shot noise variance is

$$\sigma_s^2 = 2q\langle M\rangle^2 F_A R P_{\text{rec}} \Delta f_{\text{elec}}, \tag{3}$$

where q is the electron charge and Δf_{elec} is the receiver electrical bandwidth.[9,10] For our calculations, the electrical bandwidth was matched to the signal pulse width τ, $\Delta f_{\text{elec}} = 1/\tau$, to maximize SNR.[19,20] F_A is the excess noise figure (NF), which is related to statistical fluctuations in the APD gain, and is given as

$$F_A = k\langle M\rangle + (1-k)\left(2 - \frac{1}{\langle M\rangle}\right), \tag{4}$$

where k is the ionization coefficient ratio, a ratio between the ionization rate of holes and electrons.[7,9,21]

The thermal noise variance is given as

$$\sigma_t^2 = 4k_{\text{B}}T/R_L \Delta f_{\text{elec}}, \tag{5}$$

where k_{B} is Boltzmann's constant, T is temperature, and R_L is the load resistance.[9,10] In APDs, the thermal noise variance and receiver bandwidth are both inversely proportional to the load resistance. This creates a trade-off between noise and bandwidth. For high speed APDs, a 50 Ω load is typical; for lower bandwidth APDs, higher resistance loads are common.[22–24]

The SNR performance of an example APD is shown in Fig. 2, using parameters that correspond to case A in Table 1. In APDs, both signal and shot noise are gain dependent; this creates a nonlinear relationship between the APD gain and SNR, as shown in Fig. 2(a). As a result, there exists an optimum gain for which the SNR is maximized. This optimum APD gain and its corresponding SNR are dependent on the received optical power, as shown in Fig. 2(b). Since received power varies between measurements and APD gain is usually fixed on a sample-to-sample basis, this will lead to nonuniform system performance. Systems are often optimized for their worst-performance case. Therefore, in LiDAR, the APD gain should be optimized for the farthest target, which corresponds to the lowest average received power.

The ionization coefficient ratio of an APD also has a critical impact on SNR by affecting how the excess NF scales with gain, as shown in Eq. (4).[7,9,21] The ionization coefficient ratio is determined by the material composition and structure of the APD. At 1550 nm, InGaAs APDs are the most popular with ionization coefficient ratios ranging from 0.4 to 0.2 for InP and InAlAs

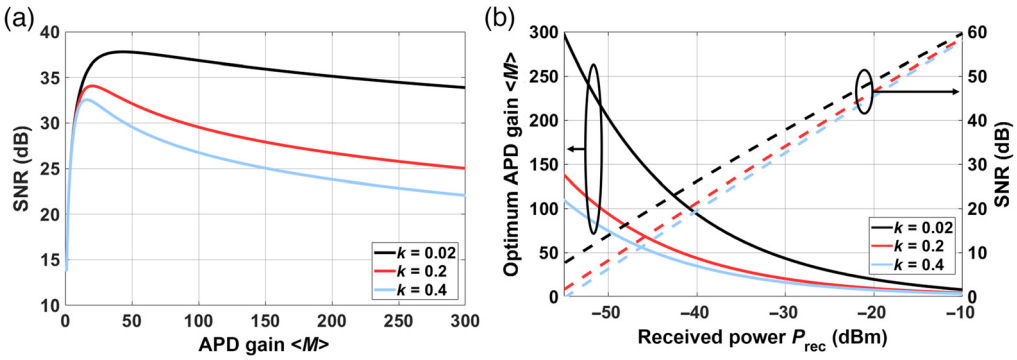

Fig. 2 (a) APD SNR increases with APD gain $\langle M\rangle$ until an optimum gain after which SNR decreases. Results shown for $P_{\text{rec}} = -30$ dBm and $\tau = 5$ ns. (b) The SNR, and optimum gain, depends on the received power P_{rec} and ionization coefficient ratio k.

Table 1 Calculation parameters. Case A corresponds to ideal parameters; cases B and C are practical parameters.

	Parameter	Unit	Value	References
Signal	Pulse width (τ)	ns	5	
	Wavelength (λ)	nm	1550	
APD	Load resistance (R_L)	Ohms	50	22–24
	Responsivity (R_{APD})	A/W	(A) 1.25	22
			(B) and (C) 1.01	
	Gain ($\langle M \rangle$)		(A) Optimum [see Fig. 2(b)]	7
			(B) and (C) 20	
	Ionization coefficient ratio (k)		0.02, 0.2, and 0.4	7
	Temperature (T)	K	300	
Preamplified receiver	NF	dB	(A) 3	25
			(B) and (C) 4	
	Optical bandwidth ($\Delta\nu_{\mathrm{opt}}$)	GHz	(A) 0.2	26–28
			(B) 12.5	
			(C) 37.5	
	Number of modes ($2m_t$)		20, 40, and 60	

multipliers, respectively, to 0.02 for multiple gain stages.[7] InGaAs/InP. APDs are the most common.[7] Lower ionization coefficient ratios lead to better SNR performance.

2.2 *FM Optical Preamplified Receivers*

In FM optical preamplified receivers, the received signal current is

$$I = \sum_{n=1}^{2m_t} R\, G\, P_{\mathrm{rec},n}, \tag{6}$$

where G is the optical amplifier gain, m_t is the number of transverse modes supported by the amplifier, and $P_{\mathrm{rec},n}$ is the received optical power in the n'th mode. For no polarization filtering at the receiver, the total number of modes supported by the amplifier is $2m_t$.

The effect of mode-dependent gain (MDG) is not included because FM preamplifiers with negligible MDG have been experimentally demonstrated.[29] In the presence of MDG, SNR is maximized when maximum-ratio combining is used.[30,31] However, even without maximum-ratio combining, SNR degradation is small. For example, for an optical preamplifier supporting 40 modes with mode gain uniformly distributed between 11 and 15 dB and the received power divided equally among all modes, the SNR would decrease by 0.3 dB compared with the case without MDG.

In optical preamplified receivers, stimulated emission leads to signal enhancement, and ASE produces noise. During the photodetection process, the ASE beats with the signal and itself to produce signal-ASE beat noise and ASE-ASE beat noise.

The variance of the signal-ASE beat noise is

$$\sigma^2_{\text{sig-ASE}} = \sum_{n=1}^{2m_t} 4R^2G^2P_{\text{rec},n}n_{\text{sp}}h\nu_0\Delta f_{\text{elec}}, \tag{7}$$

where $h\nu_0$ is the energy of a signal photon and n_{sp} is the inversion coefficient, a measure of the population inversion in the gain medium, which is related to the amplifier NF by $NF \approx 2n_{\text{sp}}$.[10] Like the APD, the electrical bandwidth for the preamplified receiver was matched to the signal pulse width to maximize SNR.

The variance of the ASE-ASE beat noise is

$$\sigma^2_{\text{ASE-ASE}} = \sum_{n=1}^{2m_t} 4R^2(Gh\nu_0n_{\text{sp}})^2\Delta f_{\text{elec}}\left[\Delta\nu_{\text{opt}} - \frac{\Delta f_{\text{elec}}}{2}\right], \tag{8}$$

where $\Delta\nu_{\text{opt}}$ is the optical bandwidth and is related to the electrical bandwidth via $\Delta\nu_{\text{opt}} = N\Delta f_{\text{elec}}$, where $N \geq 1$ is a multiplicative factor.[9]

From Eq. (8), ASE-ASE beat noise is independent of the received signal and is summed over the receiver modes. As such, ASE-ASE beat noise scales linearly with the number of modes $2m_t$ and leads to a decrease in the SNR as the number of modes increases, as shown in Fig. 3. Conversely, the coupling efficiency between the return speckle pattern and receiver increases with the number of receiver modes until the modal count of the two is matched. This presents a critical design consideration. To achieve maximum coupling efficiency and minimize noise, the preamplifier should be designed to match the number of modes in the receiver to that in the return speckle pattern.

The maximum number of spatial modes supported by a finite-aperture LiDAR system, and therefore in the received speckle pattern, can be found using

$$Q \leq 1.314 * M(M+1), \tag{9}$$

where $M = (\pi/4)(R * D)/\lambda L$ is the normalized space-bandwidth product, λ is the wavelength, R is the beam radius at the target, D is the receiving aperture diameter, and L is the distance to the target.[15,32] From Eq. (9), the number of modes in the received speckle pattern depends on the distance to the target. However, the number of modes supported by an optical amplifier is fixed. Therefore, the number of modes in the receiver and speckle pattern can only be matched for a single distance to the target. In LiDAR, the worst system performance will occur for targets located at the maximum range of the system.[33] The LiDAR system parameters will depend on the application. As an example though, for $L = 250$ m, $R = 4.4$ cm, and $D = 4$ cm,

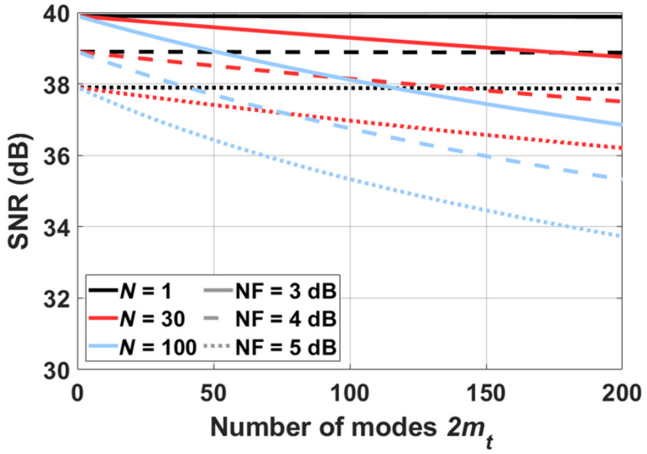

Fig. 3 FM preamplified receiver SNR decreases with increases in the number of modes supported by the amplifier $2m_t$, optical bandwidth $\Delta\nu_{\text{opt}} = Nf_{\text{elec}}$, and NF. Results are shown for $P_{\text{rec}} = -30$ dBm and $\tau = 5$ ns.

reasonable for long-range automotive LiDAR, the system will support 21 or fewer spatial modes per polarization, or 42 modes total.[7,34,35] From Fig. 3, for $2m_t = 42$, SNR decreased by 1.2 dB or less compared with the SM case. This gradual reduction in SNR with the number of modes is due to mode orthogonality, which prevents beating between different spatial modes.[15]

FM optical amplifiers offer both high coupling efficiency and minimal added noise. Comparatively, SM amplifiers only support one spatial mode, which leads to unsuitably low coupling efficiency for multimode (MM) speckle patterns, and MM amplifiers introduce excess noise in higher-order modes. Accordingly, FM optical preamplified receivers offer a critical improvement over their SM and MM predecessors for long-range LiDAR.[36]

3 Performance Comparison

In this section, we compare the performance of APDs and FM preamplified receivers for long-range LiDAR under ideal and practical conditions using the parameters listed in Table 1. We begin by discussing the receiver parameters chosen for the simulations.

Gain for commercial InGaAs APDs is generally between 2 and 40 with gain typically being below 25.[22,37,38] For the ideal case, optimum APD gain was used, as given in Fig. 2(b); for the practical case, the gain was set to $\langle M \rangle = 20$, which is typical for commercial low-noise InGaAs APDs.[7] While several novel APD architectures and compositions have been proposed, which exhibit high gain and low excess noise, these technologies are not yet mature.[39–42]

FM optical preamplified receivers are a new technology, first demonstrated in 2011, that has yet to reach full maturity.[16] As such, for the FM amplifiers, we used NF values that are typical for SM EDFAs, which are based on the same underlying physics and are a mature technology. The fundamental NF limit for EDFAs is 3 dB, whereas commercial SM EDFA preamplifiers typically have an NF between 4 and 5.5 dB.[25] To minimize noise in the preamplified receiver, the electrical and optical bandwidth should be matched. However, obtaining FM compatible bandpass filters with sufficiently narrow optical bandwidths is difficult. We calculated the performance of the FM preamplified receiver for the ideal optical bandwidth, $\Delta\nu_{\text{opt}} = \Delta f_{\text{elec}}$, an achievable 100 pm (12.5 GHz) bandwidth, and a practical bandwidth currently available in commercial off-the-shelf thin-film filters, 300 pm (37.5 GHz).[26–28]

3.1 *SNR Comparison*

Figure 4 shows the results of the SNR calculations for a 5-ns pulse width, corresponding to a range resolution of roughly 75 cm.[18] For the ideal case, shown in Fig. 4(a), FM preamplified receivers offered an SNR improvement compared with APDs over a wide range of received powers. Sensitivity is an important figure-of-merit for receivers. Receiver sensitivity represents the minimum optical power required to detect a signal, or where SNR = 1. The FM preamplified receiver with $2m_t = 40$ improved the sensitivity by 3.3, 8, and 9.5 dB compared with the APD with $k = 0.02, 0.2$, and 0.4, respectively. The optical power spectral density corresponding to the sensitivity is referred to as the noise-equivalent power (NEP) and is given as[10]

$$\text{NEP} = P_{\text{rec}}(\text{SNR} = 1)/\sqrt{\Delta f_{\text{elec}}}. \tag{10}$$

The NEP for each receiver configuration is shown in Table 2. Thermo-electrically cooling the APD to -20°C would improve the sensitivity by 0.2 dB or less.

For practical conditions and a preamplifier optical bandwidth of 100 pm, as shown in Fig. 4(b), the FM preamplified receivers still offered superior SNR to the APDs, although the advantage was smaller than for the ideal case. The FM preamplified receiver with $2m_t = 40$ improved the sensitivity by 4.5 and 4.6 dB compared with the APDs with $k = 0.02, 0.2$, and 0.4. When the FM preamplifier optical bandwidth was increased to 300 pm, as shown in Fig. 4(c), the SNR advantage of the FM preamplified receivers was further reduced. In this case, the FM preamplified receiver with $2m_t = 40$ only improved the sensitivity by ~2 dB compared with the APDs. Whether preamplified receivers offer an SNR improvement over APDs will depend heavily on the LiDAR system parameters.

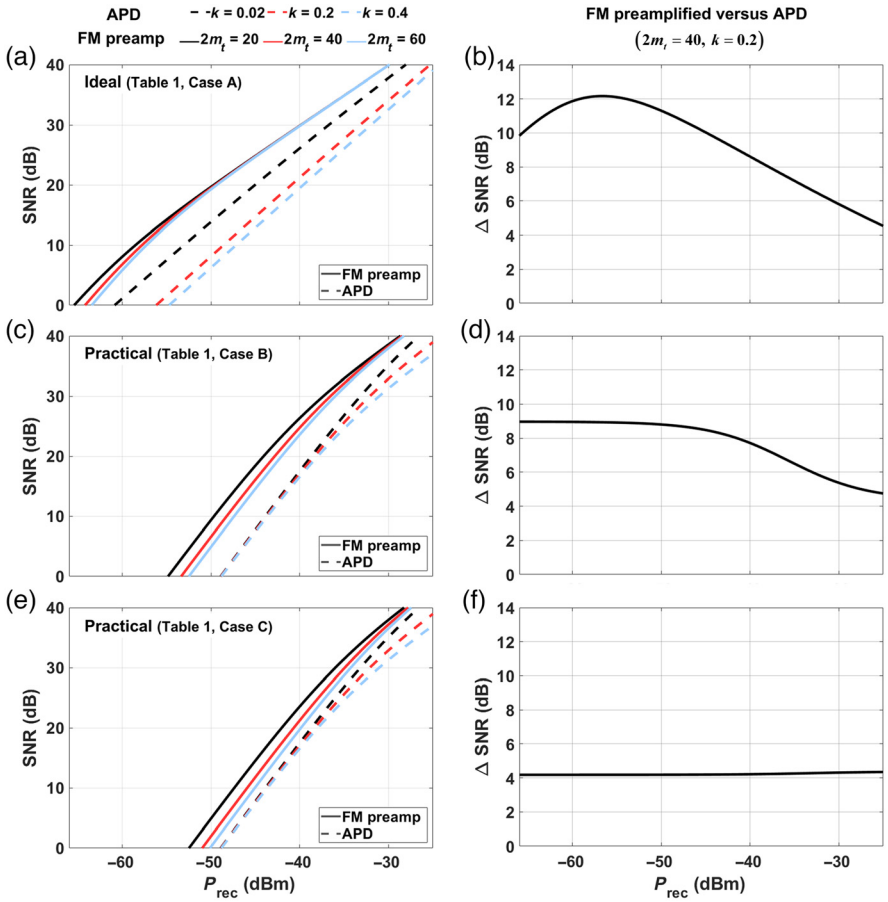

Fig. 4 SNR of FM preamplified receivers and APDs with (a) ideal and (c) and (e) practical receiver parameters for a preamplifier optical bandwidth of (c) 100 pm and (e) 300 pm. (b), (d), and (f) The corresponding SNR difference between the FM preamplified receiver with $2m_t = 40$ and the APD with $k = 0.2$. The FM preamplified receivers offer superior SNR to the APDs.

Table 2 NEP for APDs and FM optical preamplified receivers.

	Parameters	NEP
APD	$\langle M \rangle$ = optimum, $k = 0.02$	58 fw/$\sqrt{\text{Hz}}$
	$k = 0.2$ (a)	170 fw/$\sqrt{\text{Hz}}$
	$k = 0.4$	240 fw/$\sqrt{\text{Hz}}$
	(b) and (c) $\langle M \rangle = 20$, $k = 0.02$	911 fw/$\sqrt{\text{Hz}}$
	$k = 0.2$	911 fw/$\sqrt{\text{Hz}}$
	$k = 0.4$	932 fw/$\sqrt{\text{Hz}}$
Preamplified receiver	$\Delta\nu_{\text{opt}} = 2$ GHz, $2m_t = 20$	20 fw/$\sqrt{\text{Hz}}$
	$2m_t = 40$ (a)	27 fw/$\sqrt{\text{Hz}}$
	$2m_t = 60$	32 fw/$\sqrt{\text{Hz}}$
	$\Delta\nu_{\text{opt}} = 12.5$ GHz, $2m_t = 20$	229 fw/$\sqrt{\text{Hz}}$
	$2m_t = 40$ (b)	323 fw/$\sqrt{\text{Hz}}$
	$2m_t = 60$	398 fw/$\sqrt{\text{Hz}}$
	$\Delta\nu_{\text{opt}} = 37.5$ GHz, $2m_t = 20$	398 fw/$\sqrt{\text{Hz}}$
	$2m_t = 40$ (c)	562 fw/$\sqrt{\text{Hz}}$
	$2m_t = 60$	691 fw/$\sqrt{\text{Hz}}$

Note that the SNR spread of the FM preamplified receivers with different numbers of modes was smaller for ideal parameters than for practical conditions. Under ideal conditions, ASE is minimized. Since ASE-ASE beat noise scales with the number of modes, this reduces the variation in noise with number of modes. Therefore, mode number optimization is less critical for optical amplifiers with near ideal parameters. By contrast, the differences in SNR were larger for APDs with different ionization coefficient ratios under ideal conditions than practical conditions at low received powers because optimum gain varies greatly between the APDs. For the practical cases, fixed gain led to similar SNR performance at low received power for all the APDs.

4 High-Bandwidth LiDAR

One of the main advantages of optical preamplified receivers compared with APDs is their bandwidth. EDFA performance is largely data rate invariant.[10] As such, in EDFA preamplified receivers, the receiver bandwidth is limited not by the amplification process, but by the speed of the photodetector. Optical preamplified receivers can use PIN photodiodes as their detector. PIN photodiodes offer higher bandwidths than APDs, are readily available with bandwidths larger than 10 GHz, and are low cost.[9]

By contrast, APD bandwidth is limited by its fixed gain-bandwidth product.[8] High APD gain is required for optimum SNR performance in long-range LiDAR, as shown in Fig. 2(b). This requirement places a stringent upper bound on the achievable APD bandwidth. The largest bandwidth currently available for commercial high-gain $(\langle M \rangle > 20)$, low-noise $(k < 0.2)$ InGaAs APDs is 2.3 GHz.[22] While larger bandwidths have been measured for high-gain APDs in the lab, these APDs are not commercially available.[39–42]

High bandwidth receivers enable a number of useful features for long-range LiDARs, such as high-spatial resolution and unique pulse identification. In this section, we detail LiDAR receiver bandwidth requirements based on desired measurement resolution and identification requirements.

4.1 *Measurement Resolution*

The required LiDAR system resolution will depend on the application. We describe the resolution requirements of long-range automotive LiDAR as an illustrative example. Measurement resolution will determine the system sampling rate and thereby the required receiver bandwidth.

Three factors contribute to the sampling rate of a LiDAR system: angular resolution, field-of-view (FOV), and frame rate. Commercial automotive LiDAR systems offer angular resolutions between 0.02 deg and 1.33 deg and it is expected that long-range automotive LiDAR will require an angular resolution of 0.1 deg or better.[7,43–45] For FOV, automotive LiDAR must cover all 360 deg in the horizontal direction, although this can be accomplished using a group of LiDAR modules, and 40 deg in the vertical direction.[7,45] Finally, frame rates from 1 to 100 Hz are available in commercial LiDAR systems, although a frame rate of 20 Hz or greater is desirable.[32,45,46] As an example long-range automotive LiDAR system, for an angular resolution of 0.05 deg, a FOV of 120 deg by 40 deg, and a frame rate of 20 Hz, the sampling rate would be 38.4 MHz. However, commercial automotive LiDAR systems typically offer sampling rates between hundreds of kHz to a couple MHz, at least an order of magnitude lower than the aforementioned desired sampling rate.[2] While the desired sampling rate of 38.4 MHz is within the bandwidth capabilities of APDs, an issue arises with the unambiguous rate.

In traditional scanning pulsed LiDAR, the pulses are identical, therefore only one pulse can be measured at a time to prevent misidentifying pulses. This single-pulse requirement limits the sampling rate to the inverse of the maximum round trip time. This upper bound on the sampling rate, known as the unambiguous rate, is given as

$$f_{\text{unamb}} = \frac{c}{2L_{\max}}, \tag{11}$$

where $L_{\max}$ is the maximum distance to a target. Typical long-range LiDAR systems are designed to work for between 150 to 400 m, corresponding to an unambiguous rate of

1 MHz to 375 kHz.[7] Therefore, the unambiguous rate is lower than the sampling rate required to achieve the desired spatial resolution.

4.2 *Pulse Identification*

One solution to overcome the unambiguous rate is to remove pulse identity ambiguity by creating each pulse with unique characteristics. This allows LiDAR systems to use more than one pulse at a time. Optical code-division multiple-access (OCDMA) with optical orthogonal codes is one method that has been used to uniquely identify pulses in LiDAR.[47–50] In this method, each LiDAR pulse is converted into a unique sequence of micropulses.[47]

Since these shorter micropulses must be accurately measured, OCDMA places additional bandwidth requirements on the receiver. To calculate the additional bandwidth required, the number of pulses simultaneously in the air must be determined. This number is given as

$$N_{\text{pulse}} = \frac{f_{\text{samp}}}{f_{\text{unamb}}}, \tag{12}$$

where f_{samp} is the desired sampling rate. For measuring an object that is 250 m from the LiDAR system at a sampling rate of 38.4 MHz, 64 pulses will exist simultaneously between the transmitter and receiver. Therefore, the LiDAR system must be capable of distinguishing 64 pulses.

In OCDMA, the number of unique sequences C, or identifiable pulses, is given as

$$C \leq \left\lfloor \frac{F-1}{K(K-1)} \right\rfloor, \tag{13}$$

where F is the sequence length or the number of micropulses and K is the sequence weight or the number of ones within the sequence.[50] For 64 unique pulses, this leads to a minimum sequence length of 129, corresponding to each LiDAR pulse consisting of 129 micropulses. Therefore, a bandwidth of ~5 GHz would be required, a factor of 2 greater than the largest bandwidth offered by a commercial high-gain, low-noise InGaAs APD. This necessitates the use of other, higher-bandwidth, receivers.

In addition, unique pulse identification allows a LiDAR system to distinguish between pulses from itself and foreign sources, such as neighboring LiDAR systems or attackers.[47,50] The required code length, and thereby bandwidth, would be even greater if pulses from other sources were considered in this calculation.

5 Conclusions and Discussion

FM optical preamplified receivers can be used in long-range pulsed scanning LiDAR to increase bandwidth while offering improved or comparable SNR performance to LM APDs. FM preamplified receivers are best suited for LiDAR applications that require a high-sampling rate or high-resolution and where the number of modes in the return speckle pattern is low. To optimize performance, the FM EDFA should be designed with the expected return optical power in mind. In particular, the doping concentration, active fiber length, and pump power should be optimized for amplifying the weakest input signal.[51] Techniques, such as multistage amplification and implementing narrow linewidth optical bandpass filters, can also be implemented to ensure that the EDFA has a low NF.[51–53]

FM optical preamplifiers are an area of active research within telecommunications.[54] The first laboratory demonstration of FM EDFAs occurred in 2011; By 2014, devices were available commercially.[16,55] The rapid development and commercialization of FM EDFAs has benefitted from building off of the well-established, heavily deployed, and robust technology of SM EDFAs.[25] LiDAR systems with an operating wavelength of 1550 nm are well-poised to take advantage of advances in FM EDFAs for telecommunications.

While the optical preamplifiers discussed in this paper focused on fiber-based EDFAs, Wen et al.[56] recently demonstrated an FM semiconductor optical amplifier (SOA). The SOAs are

an attractive alternative to EDFAs because they allow for on-chip receivers that would be readily compatible with solid-state LiDAR systems. However, further improvements in the NF of SOAs are necessary for comparable performance to EDFAs.[9]

Acknowledgments

This research was supported by the National Science Foundation (Grant Nos. 1649522 and 1808976). The authors declare no conflicts of interest.

References

1. Frost & Sullivan, *LiDAR: Driving the Future of Autonomous Navigation—Analysis of LiDAR Technology for Advanced Safety* (2016).
2. Woodside Capital Partners and Yole Development, *Automotive LiDAR Market REPORT* (2018).
3. M. Flood, "Laser altimetry: from science to commercial LiDAR mapping," *Photogramm. Eng. Remote Sens.* **67**, 1209–1217 (2001).
4. B. Schwarz, "Mapping the world in 3D," *Nat. Photonics* **4**, 429–430 (2010).
5. S. Piatek, "LiDAR and other techniques: measuring distance with light for automotive industry," in *Sens. Expo and Conf.* (2018).
6. S. Royo and M. Ballesta-Garcia, "An overview of LiDAR imaging systems for autonomous vehicles," *Appl. Sci.* **9**(19), 4093 (2019).
7. G. M. Williams, "Optimization of eyesafe avalanche photodiode LiDAR for automobile safety and autonomous navigation systems," *Opt. Eng.* **56**(3), 031224 (2017).
8. E. B. Emmons, "Avalanche-photodiode frequency response," *Appl. Phys.* **38**, 3705–3714 (1967).
9. M. Cvijetic and I. B. Djordjevic, *Advanced Optical Communication Systems and Networks*, Artech House, Norwood, MA, (2013).
10. G. Agrawal, *Fiber-Optic Communications Systems*, 4th ed., John Wiley & Sons, Hoboken, NJ (2010).
11. D. K. Killinger and A. Mooradian, Optical and Laser Remote Sensing, Springer-Verlag Berlin Hedelberg, New York (1983).
12. J. W. Goodman, "Some effects of target-induced scintillation on optical radar performance," *Proc. IEEE* **53**(11), 1688–1700 (1965).
13. J. W. Goodman, "Some fundamental properties of speckle," *J. Opt. Soc. Am.* **66**, 1145–1150 (1976).
14. R. T. Menzies, "Coherent and incoherent LiDAR—an overview," in *Tunable Solid State Lasers for Remote Sensing*, R. L. Byer, E. K. Gustafson, and R. Trebino, Eds., pp. 17–21, Springer, Berlin, (1985).
15. R. Sampson et al., "Improving the sensitivity of LiDARs using few-mode pre-amplified receivers," in *Proc. FiO/LS*, p. FW7A.2 (2018).
16. N. Bai et al., "Multimode fiber amplifier with tunable modal gain using a reconfigurable multimode pump," *Opt. Express* **19**(17), 16601–16611 (2011).
17. Y. Jung et al., "First demonstration and detailed characterization of a multimode amplifier for space division multiplexed transmission systems," *Opt. Express* **19**(26), B952–B957 (2011).
18. P. F. McManamon, *Field Guide to LiDAR*, SPIE Press, Bellingham, WA (2015).
19. A. Kilpelä, R. Pennala, and J. Kostamovaara, "Precise pulsed time-of-flight laser range finder for industrial distance measurements," *Rev. Sci. Instrum.* **72**, 2197–2202 (2001).
20. M. Hintikka and J. Kostamovaara, "Time domain characterization of avalanche photo detectors for sub-ns optical pulses," in *Proc. IEEE Int. Instrum. Meas. Technol. Conf.* (2015).
21. R. J. McIntyre, "Multiplication noise in uniform avalanche diodes," *IEEE Trans. Electron Devices* **ED-13**(1), 164–168, (1966).
22. Voxtelopto, *Photodiodes, APDs, Photoreceivers, LRF Receivers, Electro-Optical Instruments* (2015).

23. R. Hui, *Introduction to Fiber-Optic Communications*, Academic Press (2019).
24. Solid State Division, Hamamatsu Photonics K.K., *Opto-Semiconductor Handbook* (2014).
25. Finisar, *Introduction to Optical Amplifiers* (2010).
26. Barr Associates, *Ultra-Narrow Bandpass Filters* (2003).
27. M. A. Fredell et al., "Sub-nanometer band pass coatings for LiDAR and astronomy," *Proc. SPIE* **9612**, 96120K (2015).
28. OzOptics, *Fixed Filters* (2015).
29. H. A. Youssef, Z. A. El-Sahn, and A. A. El-Zoghabi, "Performance of few-mode EDFAs in optical space-division multiplexed communication systems," in *Proc. Asia Commun. and Photonics Conf. (ACP)*, p. ATh3A.81 (2014).
30. H. Liu et al., "Turbulence-resistant FSO communication using a few-mode pre-amplified receiver," *Sci. Rep.* **9**, 16247 (2019).
31. L. R. Kahn, "Ratio squarer," *Proc. IRE (Corresp.)* **42**(11), 1698–1704 (1954).
32. N. Zhao et al., "Capacity limits of spatially multiplexed free-space communication," *Nat. Photonics* **9**, 822–826 (2015).
33. P. McManamon, "Review of ladar: a historic, yet emerging, sensor technology with rich phenomenology," *Opt. Eng.* **51**(6), 060901 (2012).
34. J. Hecht, "LiDAR for self-driving cars," *Opt. Photonics News* **29**, 26–33 (2018).
35. P. E. Ross, "Luminar's LiDAR enters mass production," *IEEE Spectr.* (2018).
36. H. P. Chou et al., "Eye-safe LiDAR receiver using Er^{3+}: fiber optical preamplifier," *Proc. SPIE* **3000**, 72–81 (1997).
37. Discovery Semiconductors, DSC-402APD: 10 Gb/s APD+TIA optical receiver, Discovery Semiconductors Inc. (2002).
38. D. G. Youmans, G. M. Williams, and A. S. Huntington, "Linear-mode avalanche photodiode detectors with a quasi-deterministic gain component: statistical model studies," *Proc. SPIE* **8037**, 803716 (2011).
39. S. Xie et al., "InGaAs/AlGaAsSb avalanche photodiode with high gain-bandwidth product," *Opt. Express* **24**(21), 24242–24247 (2016).
40. A. R. J. Marshall et al., "High speed InAs electron avalanche photodiodes overcome the conventional gain-bandwidth product limit," *Opt. Express* **19**(23), 23341–23349 (2011).
41. N. Duan et al., "310 GHz gain-bandwidth product Ge/Si avalanche photodetector for 1550 nm light detection," *Opt. Express* **20**(10), 11031–11036 (2012).
42. G. M. Williams et al., "Multi-gain-stage InGaAs avalanche photodiode with enhanced gain and reduced excess noise," *IEEE J. Electron Devices Soc.* **1**(2), 54–65, (2013).
43. G. Overton, "Insight LiDAR announces FMCW LiDAR Sensor for autonomous vehicles," *Laser Focus World* (2019).
44. Velodyne LiDAR, *HDL-32E: High Definition LiDAR Sensor: User's Manual and Programming Guide* (2015).
45. R. Mardirosian, "What matters in LiDAR," in *Auton. Veh. Sens. Conf.* (2018).
46. LeddarTech, *Leddar Vu8: 8-Segement Solid-State LiDAR Sensor Module* (2018).
47. T. Fersch, R. Weigel, and A. Koelpin, "A CDMA modulation technique for automotive time-of-flight LiDAR systems," *IEEE Sens. J.* **17**(11), 3507–3516 (2017).
48. G. Kim and Y. Park, "LiDAR pulse coding for high resolution range imaging at improved refresh rate," *Opt. Express* **24**(21), 23810–23828 (2016).
49. G. Kim and Y. Park, "Independent biaxial scanning light detection and ranging system based on coded laser pulses without idle listening time" *Sensors* **18**(9), 2943 (2018).
50. J. A. Salehi, "Code division multiple-access techniques in optical fiber networks—part I: fundamental principles," *IEEE Trans. Commun.* **37**(8), 824–833 (1989).
51. A. Cem Cokrak and A. Altuncu. "Gain and noise figure performance of erbium doped fiber amplifiers (EDFA)," *J. Electr. Electron. Eng.* **4**(2), 1111–1122 (2004).
52. J.-M. P. Delavaux and J. A. Nagel, "Multi-stage erbium-doped fiber amplifier designs," *J. Lightwave Technol.* **13**(5), 703–720 (1995).
53. J. M. Roth et al., "Single-polarization optical low-noise pre-amplified receiver for heavily coded optical communications links," *Proc. SPIE* **9354**, 935409 (2015).

54. B. J. Puttnam, G. Rademacher, and R. S. Luís, "Space-division multiplexing for optical fiber communications," *Optica* **8**, 1186–1203 (2021).
55. J. Wallace, "European MODE-GAP project commercially launches few-mode fiber erbium-doped amplifier," *Laser World Focus* (2014).
56. H. Wen et al., "Four-mode semiconductor optical amplifier," *APL Photonics* **1**, 070801 (2016).

Rachel Sampson received her MS degree in optics from CREOL, The College of Optics and Photonics, University of Central Florida. She is currently a technical staff member at MIT Lincoln Laboratory and a PhD candidate in the optics program at the University of Central Florida. Her research interests include LiDAR and free-space optical and fiber optic communications. She received the NSF Graduate Research Fellowship and Order of Pegasus Award.

Huiyuan Liu: Biography is not available.

Guifang Li received his PhD from the University of Wisconsin—Madison. He is a professor of Optics and Electrical and Computer Engineering at the University of Central Florida. His research interests include optical communication and networking, RF photonics, all-optical signal processing, and imaging. He is a fellow of the National Academy of Inventors, IEEE, The Optical Society, and SPIE. He currently serves as the editor-in-chief of *Advances in Optics and Photonics*.